D-501036, a novel selenophene-based triheterocycle derivative, exhibits potent *in vitro* and *in vivo* antitumoral activity which involves DNA damage and ataxia telangiectasia–mutated nuclear protein kinase activation

Shin-Hun Juang,[1] Chia-Chi Lung,[2] Pi-Chen Hsu,[3] Kuo-Shun Hsu,[2] Yu-Chen Li,[3] Pao-Chiung Hong,[4] Her-Shyong Shiah,[2] Ching-Chuan Kuo,[2] Ching-Wei Huang,[3] Yu-Chin Wang,[3] Leeyuan Huang,[3] Tom S. Chen,[3,4] Shyh-Fong Chen,[3,4] Kuo-Chu Fu,[3] Cheng-Li Hsu,[3] Meng-Ju Lin,[3] Ching-jer Chang,[6] Curtis L. Ashendel,[6] Thomas C.K. Chan,[6] Kai-Ming Chou,[7] and Jang-Yang Chang[2,5]

[1]School of Pharmacy, China Medical University and the Department of Medical Research, China Medical University Hospital, Taichung; [2]Institute of Cancer Research, National Health Research Institutes; Departments of [3]Pharmacology and [4]Medicinal Chemistry, Development Center for Biotechnology; [5]Division of Hematology/Oncology, Tri-Service General Hospital, National Defense Medical Center, Taipei, Taiwan, Republic of China; [6]Department of Medicinal Chemistry and Molecular Pharmacology, Purdue University, West Lafayette, Indiana; and [7]Cell Biology and Neuroscience Program, University of South Alabama, Mobile, Alabama

Abstract

D-501036 [2,5-bis(5-hydroxymethyl-2-selenienyl)-3-hydroxymethyl-*N*-methylpyrrole] is herein identified as a novel antineoplastic agent with a broad spectrum of antitumoral activity against several human cancer cells and an IC_{50} value in the nanomolar range. The IC_{50} values for D-501036 in the renal proximal tubule, normal bronchial epithelial, and fibroblast cells were > 10 μmol/L. D-501036 exhibited no cross-resistance with vincristine- and paclitaxel-resistant cell lines, whereas a low level of resistance toward the etoposide-resistant KB variant was observed. Cell cycle analysis established that D-501036 treatment resulted in a dose-dependent accumulation in S phase with concomitant loss of both the G_0-G_1 and G_2-M phase in both Hep 3B and A-498 cells. Pulsed-field gel electrophoresis showed D-501036–induced, concentration-dependent DNA breaks in both Hep 3B and A-498 cells. These breaks did not involve interference with either topoisomerase-I and topoisomerase-II function or DNA binding. Rapid reactive oxygen species production and formation of Se-DNA adducts were evident following exposure of cells to D-501036, indicating that D-501036–mediated DNA breaks were attributable to the induction of reactive oxygen species and DNA adduct formation. Moreover, D-501036–induced DNA damage activated ataxia telangiectasia–mutated nuclear protein kinase, leading to hyperphosphorylation of Chk1, Chk2, and p53, decreased expression of CDC25A, and up-regulation of $p21^{WAF1}$ in both p53-proficient and p53-deficient cells. Collectively, the results indicate that D-501036–induced cell death was associated with DNA damage–mediated induction of ataxia telangiectasia–mutated activation, and p53-dependent and -independent apoptosis pathways. Notably, D-501036 shows potent activity against the growth of xenograft tumors of human renal carcinoma A-498 cells. Thus, D-501036 is a promising anticancer compound that has strong potential for the management of human cancers. [Mol Cancer Ther 2007;6(1):193–202]

Introduction

Naturally occurring substances have proven to be fruitful anticancer agents. Major anticancer drugs that include bleomycin, doxorubicin, mitomycin, vinblastine, vincristine, etoposide (VP16), topotecan, irinotecan, and paclitaxel are natural products or their derivatives (1). ''Lou-Lu'' is one of the most widely used Chinese traditional medicines for the relief of heat stress; the compound is also used in a combination prescription for treating lung, liver, and breast cancer. Screening for potential antitumor agents in the alcoholic extracts of *Echinops grijsii* has identified α-terthiophene as a potent protein kinase C (PKC)–α and PKC-β2 inhibitor, displaying a concentration that inhibited 50% of enzyme activity (IC_{50}) with <1 μmol/L (2). Furthermore, examination of synthetic derivatives of α-terthiophene has established that some derivatives displayed marked cytotoxicity against renal and ovarian tumors in the National Cancer Institute human tumor panels (3).

Received 8/10/06; revised 10/17/06; accepted 11/22/06.

Grant support: CA-095-PP-04 of National Health Research Institutes, Taipei and National Science Council (NSC-94-2752-B-400-001-PAE and NSC-95-2320-B-039-034-MY2), Taipei, Taiwan, ROC.

The costs of publication of this article were defrayed in part by the payment of page charges. This article must therefore be hereby marked *advertisement* in accordance with 18 U.S.C. Section 1734 solely to indicate this fact.

Note: S-H. Juang and C-C. Lung contributed equally to this work.

Requests for reprints: Jang-Yang Chang, Institute of Cancer Research, National Health Research Institutes, 7th Floor, No. 161, Section 6, Min-Chuan East Road, Taipei 114, Taiwan, Republic of China. Phone: 886-2-2792-9682; Fax: 886-2-2792-9654. E-mail: jychang@nhri.org.tw

doi:10.1158/1535-7163.MCT-06-0482

Trace mineral selenium and selenium-containing compounds have shown that they could induce apoptotic death and inhibit tumor growth (4). Because sulfur and selenium belong to the same group (group VIA), thiophene-based compounds should be able to replace the sulfur molecule with a selenium molecule, generating novel selenophene derivatives as a new class of anticancer drugs. Therefore, the benefits of replacing the sulfur molecule with selenium for enhanced antitumor ability and stability of polythiophene has been studied. Substitution of selenium with a sulfur molecule does not significantly improve the solubility and stability of polyselenothiophene compounds. However, we have found that the introduction of *N*-methylpyrrole and one or more hydroxymethyl groups to the original selenophene-containing polythiophene heteroarene can improve their stability and solubility without compromising anticancer potency.[8] One of these compounds is 2,5-bis(5-hydroxymethyl-2-selenienyl)-3-hydroxymethyl-*N*-methylpyrrole (D-501036). D-501036 was identified as a potent cytotoxic agent with good solubility and stability and was thus chosen for further development. In the present study, we investigated the molecular mechanism(s) of action of D-501036 and examined whether its efficacy was affected by multidrug resistance status in selected cancer cell lines. Moreover, *in vivo* antitumor activities against human xenografts were also evaluated in murine preclinical models.

Materials and Methods

Reagents

Monoclonal antibodies against phospho-ATM (serine 1981), phospho-p53 (serine 15), phospho-Chk1 (serine 317), and phospho-Chk2 (threonine 68) were purchased from Cell Signaling Technology (Beverly, MA). Antibody against $p21^{WAF1}$ was purchased from Lab Vision Co. (Westinghouse, CA), monoclonal antibody for α-tubulin was purchased from Sigma-Aldrich (St. Louis, MO), and horseradish peroxidase–conjugated secondary antibody was purchased from Santa Cruz Biotechnology (Santa Cruz, CA). Cell culture reagents were obtained from Life Technologies (Gaithersburg, MD). PKC-α and PKC-β2 were purchased from Calbiochem (San Diego, CA). Acrylamide, bisacrylamide, ammonium persulfate, and *N,N,N′,N′*-tetramethylethylene diamine were obtained from Bio-Rad (Richmond, CA). 3-(4,5-Dimethythiazol-2-yl)-5-(3-carbomethoyphenyl)-2-(4-sulfophenyl)-2H-tetrazolium was obtained from Promega (Madison, WI). Dichlorofluorescein diacetate was purchased from Molecular Probes (Eugene, OR). Western blot chemiluminescence reagent was purchased from Perkin-Elmer Life Sciences (Boston, MA). FCS was purchased from Bio Whittaker (Walkersville, MD). All of the other chemicals were from Sigma-Aldrich or E. Merck Co. (Darmstadt, Germany) and were standard analytical grade or higher.

[8] Hong et al., personal communication.

Synthesis of D-5001036

D-501036 was synthesized at the Department of Medicinal Chemistry, Development Center for Biotechnology, Taipei, Taiwan, Republic of China. Briefly, the α-terheteroarene core structure was synthesized by Paal-Knorr condensation of 1,4-bis(2′-selenienyl)buta-1,4,-dione with methyl ammonium chloride. The BuL/DMF condensation method was used for the preparation of the intermediate with aldehyde functional groups at the α-positions of the selenophene rings. The 3′-CHO group of the central pyrrole ring was selectively introduced by Vilsmeier reaction and followed by reduction to obtain the final product. The substance was recrystallized from acetone/hexane. The structure of D-501036 is depicted in Table 1; this structure was verified by ^{1}H-NMR and ^{13}C-NMR.

Cell Lines

Eight human cancer cell lines including hepatocellular carcinoma Hep 3B, renal carcinoma A-498, breast carcinoma MCF-7, non–small cell lung carcinoma NCI-H460, prostate carcinoma LNCaP, colorectal carcinoma HT-29, and cervical carcinoma KB cells were obtained from American Type Culture Collection (Rockville, MD). The KB cell line was originally believed to be derived from an epidermal

Table 1. Growth inhibition of D-501036 against human cancer and normal cell lines

Cell	Description	IC_{50}
Human cancer cells		(nmol/L)
Hep 3B	Hepatocellular carcinoma	15.4 ± 6.0
A-498	Kidney carcinoma	9.1 ± 2.7
MCF-7	Breast carcinoma	5.9 ± 1.9
NPC-TW01	Nasopharyngeal carcinoma	16.6 ± 2.1
NCI-H460	Non–small cell lung carcinoma	3.5 ± 1.1
LNCaP	Prostate carcinoma	51.0 ± 5.7
HT-29	Colorectal carcinoma	157 ± 15.7
KB*	Cervical carcinoma	466.7 ± 80.4
Human normal cells		(μmol/L)
RPTEC	Renal proximal tubule epithelial cell	>10
NHBE	Bronchial/tracheal epithelial cell	>10
Detroit 551	Skin fibroblast	>10

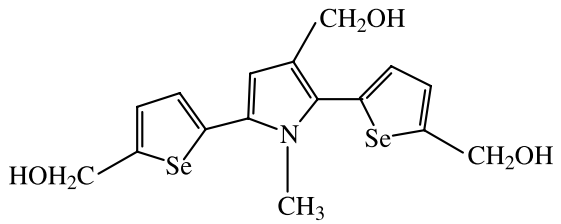

NOTE: Cells were treated with various concentrations of D501036 for 72 h. Cell survival was determined by 3-(4,5-dimethythiazol-2-yl)-5-(3-carbomethoyphenyl)-2-(4-sulfophenyl)-2H-tetrazolium assay. Each IC_{50} value was calculated as described in Materials and Methods. Each value represents the mean ± SD of three independent experiments.

*The KB cell line was originally believed to be derived from an epidermal carcinoma of the mouth but has now been shown to have HeLa characteristics.

carcinoma of the mouth but has been shown to have HeLa characteristics. Nasopharyngeal carcinoma NPC-TW01 was purchased from the Taiwan Food Industry Research and Development Institute, Hsinchu, Taiwan, Republic of China. Normal human skin fibroblast Detroit 551 was obtained from American Type Culture Collection. All the tumor cell lines and normal fibroblast cells were maintained in either RPMI 1640 or DMEM supplied with 10% fetal bovine serum at 37°C in a humidified atmosphere of 5% CO_2/95% air in the absence of antibiotics. Two normal human cell lines [renal proximal tubule epithelial (RPTEC) cells and bronchial/tracheal (NHBE) cells] were obtained from Cambrex Corporation (East Rutherford, NJ) and were maintained in REGM BulletKit at 37°C in a humidified atmosphere of 5% CO_2/95% air, in the absence of antibiotics, according to the manufacturer's recommendation. KB-derived drug-resistant cell lines KBvin10, KBtax50, and KB-7D were maintained in RPMI 1640 supplemented with 10 nmol/L of vincristine, 50 nmol/L of paclitaxel, and 1 μmol/L of VP16, respectively. KBvin10 and KBtax50 cells were vincristine- and paclitaxel-resistant cells, respectively, and displayed overexpression of P-gp170/MDR. KB-7D cells were VP16-resistant cells, which displayed down-regulation of topoisomerase II and overexpression of multidrug-resistant protein (5). All resistant cell lines were incubated in the drug-free medium for 3 days before harvesting for growth inhibition assay.

Growth Inhibition Assay

Logarithmic phase cells were seeded in a 96-well plate and incubated overnight prior to the addition of the designated compounds. After incubation with different concentrations of the tested compounds for three doubling times, cells were incubated for 2 h with DMEM containing 0.4 mg/mL of 3-(4,5-dimethythiazol-2-yl)-5-(3-carbomethoyphenyl)-2-(4-sulfophenyl)-2H-tetrazolium; its conversion to formazan by metabolically viable cells was measured by absorbance at 490 nm in a 96-well microtiter plate reader. The percentage of conversion by mock-treated control cells was used to evaluate the effect of the chemicals on cell growth and to determine the IC_{50} concentration.

Determination of PKC-α and PKC-β2 Activity

The kinase activity of PKC-α and PKC-β2 was determined using a peptide substrate and the phosphocellulose P-81 filter method as previously described (6). The purified PKC-α and PKC-β2 kinases (15 ng/reaction) were incubated with either various concentrations of D-501036 or staurosporine for 10 min. The reaction was initiated by adding 25 μL of a reaction solution [40 mmol/L Tris-HCl (pH 7.4), 10 mmol/L $MgCl_2$, 100 μg/mL bovine serum albumin, 0.5 μCi [γ-^{33}P]ATP, and the 25 nmol/L peptide substrate (neurogranin$_{[28-43]}$)] and incubated at room temperature for 10 min. The reactions were terminated by the addition of 10 μL of the terminating solution (7.5 mol/L guanidine-HCl). Twenty microliters was withdrawn and spotted onto a P81 filter. The filters were immediately placed into a beaker containing 0.5% phosphoric acid with occasional swirling for 10 min. The papers were dried and placed in scintillation vials with 5 mL of scintillation fluid and the radioactivity was determined using a liquid scintillation counter.

Cell Cycle Analysis

Exponentially growing cells were incubated with various concentrations of D-501036 for the indicated times. The cells were then fixed, incubated with RNase, and stained with 50 μg/mL of propidium iodide. DNA content was evaluated on a Becton Dickinson (Franklin Lakes, NJ) FACScan flow cytometer and the percentage of cells in various cell cycle phases were determined by using the ModFit LT software (Verity Software House, Inc., Topsham, ME). For each analysis, 10,000 events were recorded.

DNA Fragmentation Assay

Exponentially growing cell monolayers were incubated in the presence or absence of various concentrations of D-501036 for 24 h. The nonadherent cells were collected by aspiration, and the adherent cells were harvested by trypsinization. Genomic DNA was prepared using Wizard Genomic DNA Purification Kit (Promega), according to the manufacturer's instructions. The isolated DNA samples were fractionated by electrophoresis in 1.5% agarose gels and visualized by ethidium bromide staining (0.5 μg/mL) under UV transillumination.

Determination of Caspase-3 Activity

The caspase-3 activities of D-501036–treated cells were determined using a Caspase Fluorometric Assay kit (R&D Systems, Inc., Minneapolis, MN) to detect the cleavage of the specific fluorogenic peptide substrate according to the manufacturer's instructions. Briefly, 3×10^6 cells were collected, dissolved in lysis buffer, and clarified by centrifugation. Equal amounts of the extract supernatants were incubated with 50 μmol/L of fluorescent substrate for 1 h at 37°C. The fluorescence of the cleaved substrate was determined using Victor 1420 Multilabel Counter (Wallac, Turku, Finland). The caspase-3 activity was calculated by subtracting the value obtained in the untreated sample.

Pulsed-Field Gel Electrophoresis

Both Hep 3B and A-498 cells were incubated with different concentrations of D-501036 for 24 h and collected by trypsinization, washed with PBS, and suspended in a Ficoll solution. Ficoll-suspended cells were mixed with 1% low-melting agarose solution at a final concentration of 1.25×10^6 cells per 0.1 mL of agarose block, then solidified at 4°C for 30 min. The agarose-embedded cells were lysed in 100 mmol/L of EDTA (pH 8.0), 1% sodium lauryl sarcosine, and 1 mg/mL of proteinase K for 48 h at 50°C, washed thrice with 10 mmol/L of Tris (pH 7.5), 1 mmol/L of EDTA, and 1 mg/mL of RNase A for 10 min at 37°C. The DNA agarose plugs were inserted into 1% agarose gels and DNA was separated by electrophoresis using FIGE Mapper Electrophoresis System (Bio-Rad). Electrophoresis was done at 12°C for 20 h with running conditions as follows: forward direction at 180 V, pulse time gradient from 0.1 to 12 s with a linear ramp, and reverse direction at 120 V, pulse time gradient from 0.1 to 12 s with linear ramp. After electrophoresis, DNA species were visualized by ethidium bromide staining under UV transillumination.

Measurement of Protein-Linked DNA Breaks *In vivo*

A potassium-SDS coprecipitation assay was used for the measurement of protein-linked DNA breaks (PLDB) *in vivo*, as described previously (7). Briefly, logarithmically growing Hep 3B cells were labeled with [^{14}C]-thymidine (0.5 μCi/mL) for 24 h. Cells were then treated with various concentrations of D-501036, camptothecin, and VP16 for 30 min, collected by centrifugation and lysed with prewarmed lysis buffer containing (1.25% SDS, 5 mmol/L EDTA, and 0.4 mg/mL salmon sperm DNA). Cell lysates were incubated at 65°C for 10 min; then KCl was added and chilled on ice for 10 min. The coprecipitated pellet was incubated with washing solution [10 mmol/L Tris-HCl (pH 8.0), 100 mmol/L KCl, 1 mmol/L EDTA, and 0.1 mg/mL salmon sperm DNA] at 65°C for 10 min and incubated on ice for 10 min. The supernatant was removed by centrifugation. The pellet was dissolved in water and mixed with scintillation cocktail. Radioactivity was determined by liquid scintillation spectrometry (1450 Microbeta; Wallac).

DNA Unwinding Measurements

Drug-induced DNA unwinding was assayed as described previously (8). The DNA circle-ligation assay, using linearized DNA as a substrate, was done using the method of Montecucco et al. (9).

Measurement of Fluorescence of DNA-Bound Probe

The minor groove binding effect of D-501036 was measured as described previously (10). Briefly, Hoechst 33342 at a final concentration of 4 μg/mL was added to salmon sperm DNA and the mixture was incubated at room temperature. After 10 min of incubation, different concentrations of D-501036 were added. Each mixture was incubated at room temperature for 10 min and the fluorescence derived from Hoechst 33342–bound DNA was measured fluorometrically. Netropsin and VP16 were used as positive and negative controls, respectively.

Measurement of Reactive Oxygen Species Generation

The production of cellular reactive oxygen species (ROS), mainly hydrogen peroxide, was detected by dichlorofluorescein diacetate fluorescence assay as previously described (11). In brief, cells were loaded with dichlorofluorescein diacetate at a final concentration of 5 μmol/L at 37°C for 5 min. After the addition of various concentrations of D-501036, cells were incubated at 37°C for the indicated times, then ROS generation was measured by the intensity of dichlorofluorescein fluorescence on a Becton Dickinson FACScan flow cytometer. For each analysis, 10,000 events were recorded.

Measurement of DNA Adducts in Cells

D-501036–treated cells were trypsinized and washed twice with PBS. The genomic DNA was isolated using Wizard genomic DNA isolation kit (Promega) according to the manufacturer's manual with slight modifications as described subsequently. Genomic DNA was precipitated overnight at 4°C by isopropanol. The purified DNA was dissolved in acidified double-distilled water (2% HNO_3) and the adduct formation was detected using a Perkin-Elmer ELAN 6100 DRC PLUS inductively coupled plasma–mass spectrometer. The instrument was set as follows: RF power, 1.5 kW; plasma gas flow, 17 L/min; auxiliary gas flow, 1.33 L/min; nebulizer gas flow, 0.74 L/min; lens voltage, 11.25 V; dwell time/atomic mass units, 100 ms. To avoid signal interference of the nebulizer gas Ar^{2+}, selenium was measured at 77.9173 atomic mass units and serial dilutions of a selenium standard (Merck) were used to confirm the linearity of the assay. The accumulating concentration of Se-DNA (pg of Se/μg of DNA) was calculated by subtracting the blank control.

Western Blot Analysis

Western blot analysis was done as described previously (12). Briefly, cells were treated with various concentrations of D-501036, collected by gentle scraping from the dishes, lysed in ice-cold lysis buffer [50 mmol/L Tris (pH 7.4), 0.8 mol/L NaCl, 5 mmol/L $MgCl_2$, 0.5% NP40, with protease inhibitor mixture (1 mmol/L phenylmethylsulfonyl fluoride, 1 μg/mL pepstatin, and 50 μg/mL leupeptin)], and cleared by centrifugation. The protein concentrations of the lysates were determined by using the BCA Protein Assay Reagent (Pierce Biotechnology, Rockford, IL). Proteins were separated by SDS-PAGE gels and transferred to Immobilon-P. The membranes were blocked with 5% skimmed milk for 1 h at room temperature, and incubated with different primary antibodies for 4 to 18 h at 4°C. The antibody binding was detected using the appropriate secondary antibody coupled with horseradish peroxidase according to the manufacturer's instructions. Specific antibody-labeled proteins were detected using the ECL chemiluminescence system (Amersham, Buckinghamshire, England) and visualized on Kodak X-ray film according to the manufacturer's instructions.

Animal Study

Specific pathogen–free male athymic NCr *nu/nu* mice, 6 to 8 weeks of age, were purchased from Taconic Farms (Germantown, NY). All mice were maintained in laminar airflow cabinets under specific pathogen–free conditions. A-498 cells in exponential growth were harvested by trypsin treatment and the cell viability was determined by the trypan blue exclusion method. Solitary tumors were produced by s.c. inoculation of 3×10^6 cells into the right flank region of nude mice. The tumors were allowed to grow to an average volume of 50 mm^3 [tumor volumes were calculated as $0.5 \times L$ (length) $\times H$ (height) $\times W$ (width)]; then mice were randomly grouped into three groups ($n = 8$ in each group). Tumor-implanted mice were treated thrice i.p. with vehicle (5% DMSO/10% cremophor/85% saline) or with 20 or 50 mg/kg of D-501036 every other day. Tumor size and body weight of mice were measured twice a week. At the end of the experiments, animals were euthanized with carbon dioxide inhalation, followed by cervical dislocation.

Results

Growth Inhibition of D-5001036 against Various Human Cancer Cells

To assess the growth-inhibitory activity of D-501036 towards human cancer cells, eight human cancer cell lines

from different organs were used. As shown in Table 1, hepatoma (Hep 3B), renal carcinoma (A-498), breast carcinoma (MCF-7), nasopharyngeal carcinoma (NPC-TW01), and lung cancer (NCI-H460) cells displayed the highest susceptibility to D-501036; IC_{50} values ranged from 4 to 17 nmol/L (Table 1). Cervical carcinoma (KB) and colorectal carcinoma (HT-29) cells were less susceptible to D-501036; IC_{50} ranged from 150 to 500 nmol/L. Despite this potency, D-501036 was virtually nontoxic toward normal human renal proximal tubular (RPTEC), bronchial epithelial (NHBE) cells, and skin fibroblasts (Detroit 551); IC_{50} values exceeded 10 μmol/L.

To further assess the activity of D-501036 toward cells with clinically relevant drug resistance, a series of KB-derived drug-resistant cells were examined. D-501036 exhibited no cross-resistance with vincristine (KBvin10) and paclitaxel (KBtax50)–resistant cell lines, whereas a low level of resistance toward the VP16-resistant KB-variant (KB-7D) was observed (Table 2).

Influence of D-501036 on PKC-α and PKC-β2 Enzymatic Activities

The cytotoxicity for α-terthiophene might be ascribed to its potent inhibitory activity toward PKC-α and PKC-β2 (2). Thus, we evaluated whether D-501036 could inhibit PKC-α and PKC-β2 enzymatic activities. Neither the α- nor β2-isoform of PKC enzymatic activity was inhibited by D-501036, even up to a concentration of 160 μmol/L (Fig. 1).

Influence of D-501036 on S Phase Accumulation and Apoptotic Cell Death

The effects of D-501036 on cell cycle progression of Hep 3B and A-498 cells were studied by treating cells with different concentrations of D-501036 for 24 h. D-501036 treatment resulted in a concentration-dependent accumulation in the S phase, with concomitant loss of the G_0-G_1 and G_2-M phases. In addition, a characteristic hypodiploid DNA content peak (sub-G_1) was observed both in D-501036–treated Hep 3B and A-498 cells (Fig. 2A). As shown in Fig. 2B, D-501036 induced internucleosomal DNA ladder in a concentration-dependent manner in both Hep 3B and A-498 cells. An increased caspase-3 activity was evident over time (Fig. 2C) and with increasing D-501036 concentration (data not shown) in both D-501036–treated Hep 3B and A-498 cells.

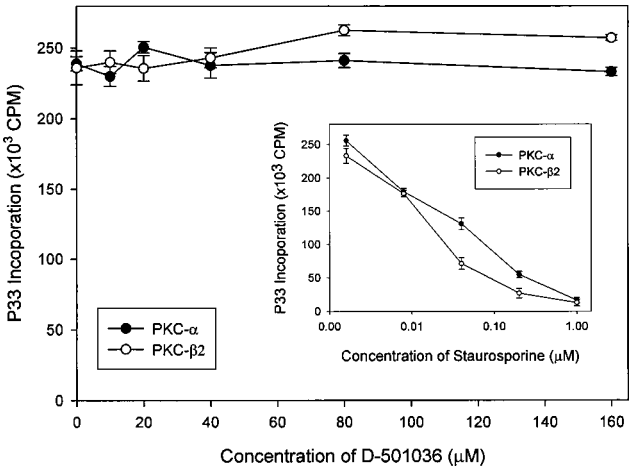

Figure 1. The effect of D-501036 on PKC-α and PKC-β2 enzymatic activity. The kinase activity of PKC-α and PKC-β2 was determined using peptide substrate and the phosphocellulose P-81 filter method as described in Materials and Methods. *Inset,* PKC enzymatic activity blocked by staurosporine as the positive control. *Points,* mean of three independent experiments; *bars,* SD.

Influence of D-501036–Mediated DNA Damage on Ataxia Telangiectasia–Mutated Nuclear Protein Kinase Signaling Pathway

Because the cell cycle analysis showed that D-501036 caused S phase accumulation and a low level resistance of D-501036 toward VP16-resistant cells was noted, pulsed-field gel electrophoresis analysis was done to determine whether D-501036 could induce DNA breaks. D-501036 caused DNA breaks in a concentration-dependent manner in both Hep 3B and A-498 cells (Fig. 3A). In contrast to the observations that both camptothecin and VP16 could generate PLDBs in a concentration-dependent manner in Hep 3B cells, no D-501036–mediated PLDB generation was observed (Fig. 3B). Moreover, the DNA breaks caused by D-501036 were not via topoisomerase-I or topoisomerase-II (data not shown).

We then determined whether D-501036 could intercalate into and/or bind to the minor groove of DNA to induce DNA breaks, using a DNA unwinding assay. A strong

Table 2. Growth inhibition of D501036 against KB-derived cancer cell lines with different resistance phenotypes

KB-derived cell lines	Resistance type	IC_{50} (nmol/L)			
		D501036	Vincristine	Paclitaxel	VP16
KB	Parental	466 ± 80	0.6 ± 0.2	4.1 ± 1.6	1.1 ± 0.2
KBvin10	MDR ↑	362 ± 93	90.1 ± 7.4	16,500 ± 707	23 ± 3.0
KBtax50	MDR ↑	323 ± 87	1.8 ± 0.5	273 ± 15	3.5 ± 0.3
KB-7D	Topoisomerase II ↓ / MDR ↑	3,200 ± 380	1.2 ± 0.4	7.9 ± 0.5	54 ± 3.5

NOTE: Cells were treated with various concentrations of the test compounds for 72 h. Cell survival was determined by 3-(4,5-dimethythiazol-2-yl)-5-(3-carbomethoyphenyl)-2-(4-sulfophenyl)-2H-tetrazolium assay. Each IC_{50} value was calculated as described in Materials and Methods. Each value represents the mean ± SD of three independent experiments.

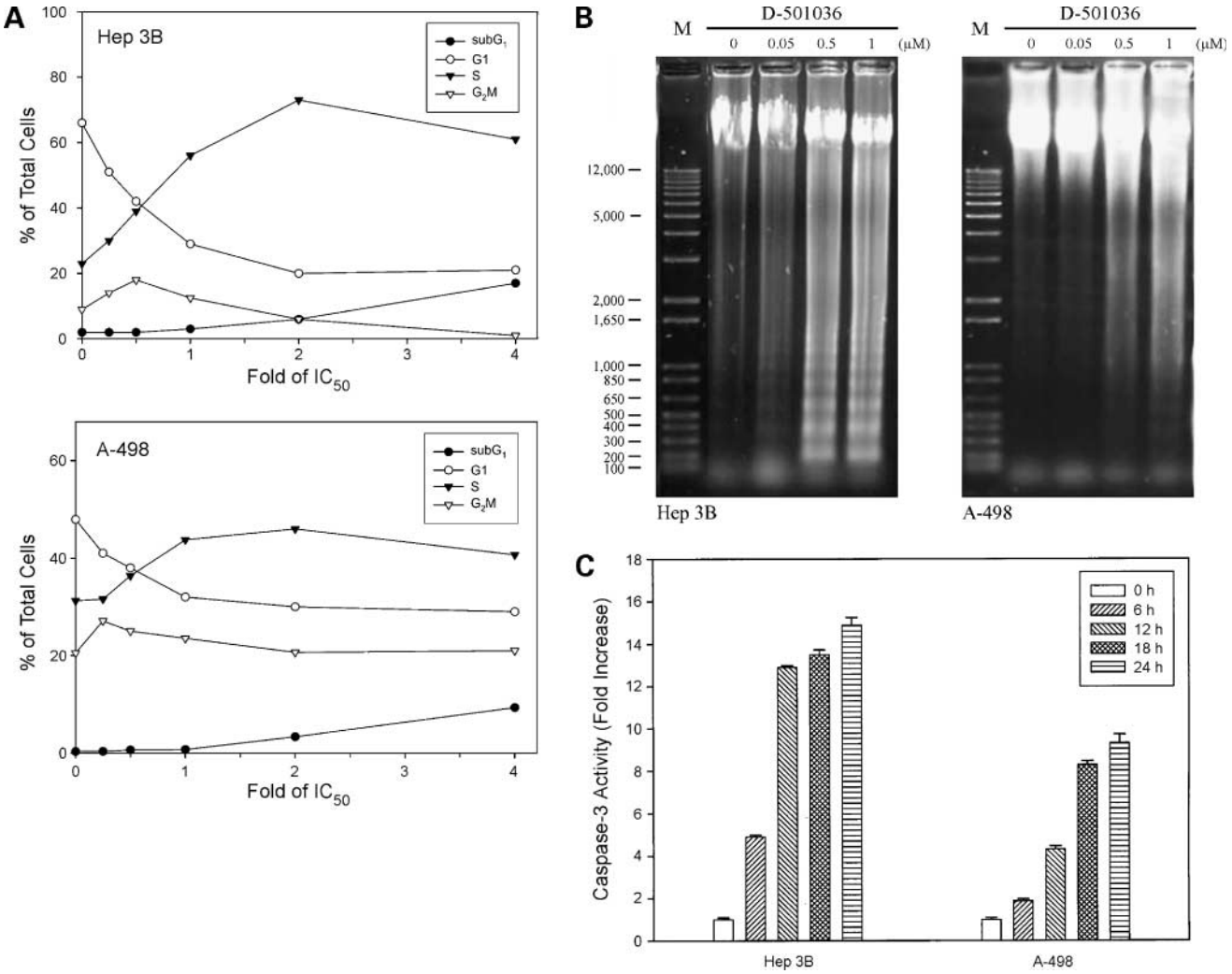

Figure 2. Effect of D-501036 on cell cycle progression and apoptotic induction of Hep 3B cells and A-498. **A,** dose effect of D-501035 on cell cycle distribution in Hep 3B and A-498 cells. **B,** DNA fragmentation in D-501036–treated Hep 3B cells and A-498. **C,** time course of Hep 3B and A-498 caspase-3 activation under 1× IC_{50} of D-501036 treatment. *Columns,* mean of three independent experiments; *bars,* SD.

DNA intercalator (Adriamycin) and a nonintercalator (camptothecin) were used as a positive or negative control, respectively. In contrast to Adriamycin, which produced a concentration-dependent DNA shift, no detectable DNA shift was observed when DNA was incubated with up to 50 μmol/L of D-501036, which was similar to the effect of camptothecin (Fig. 3C). Furthermore, the result of the Hoechst 33342 dye displacement assay showed that D-501036 was unable to quench the intensity of the fluorescence of DNA-bound Hoechst 33342, suggesting that D-501036 cannot displace Hoechst 33342 bound to DNA (Fig. 3D).

To further characterize the status and expression of DNA damage–responsive genes after D-501036 treatment, Western blot analyses were done. Ataxia telangiectasia–mutated nuclear protein kinase (ATM) was activated by D-501036 in both Hep 3B and A-498 cells (Fig. 3E). No alteration of the expression level of ATM- and Rad-3–related protein kinase was found in both Hep 3B and A-498 cells (data not shown). In addition, the phosphorylated form of Chk1 and Chk2 was increased in a dose-dependent manner in both cell lines. Furthermore, the expression levels of CDC25A, a key target protein of Chk1 and Chk2, were decreased correspondingly. We further evaluated the effect of D-501036 on the status of S phase–relative cyclin-dependent kinase inhibitor p53 and $p21^{WAF1}$. Our data showed that phosphorylated-p53 and the expression of $p21^{WAF1}$ were up-regulated in D-501036–treated A-498 cell lines. Moreover, a slight increase of $p21^{WAF1}$ expression also found in Hep 3B cells, a p53-null cell line.

D-501036 Influence on ROS Production and DNA Adduct Formation

To test whether ROS induction influences D-501036–induced DNA damage, the ROS-mediated generation of

dichlorofluorescein was used to detect the intracellular generation of ROS by D-501036. As shown in Fig. 4A, A-498 cells treated with D-501036 greatly increased the dichlorofluorescein fluorescence intensity in a concentration-dependent manner. A similar result was found in Hep 3B cells (data not shown). To further examine whether the generation of ROS is a crucial step in D-501036–induced DNA breaks, cells were treated with antioxidant prior to D-501036 treatment and then subjected to ROS production and pulsed-field gel electrophoresis analysis. As shown in

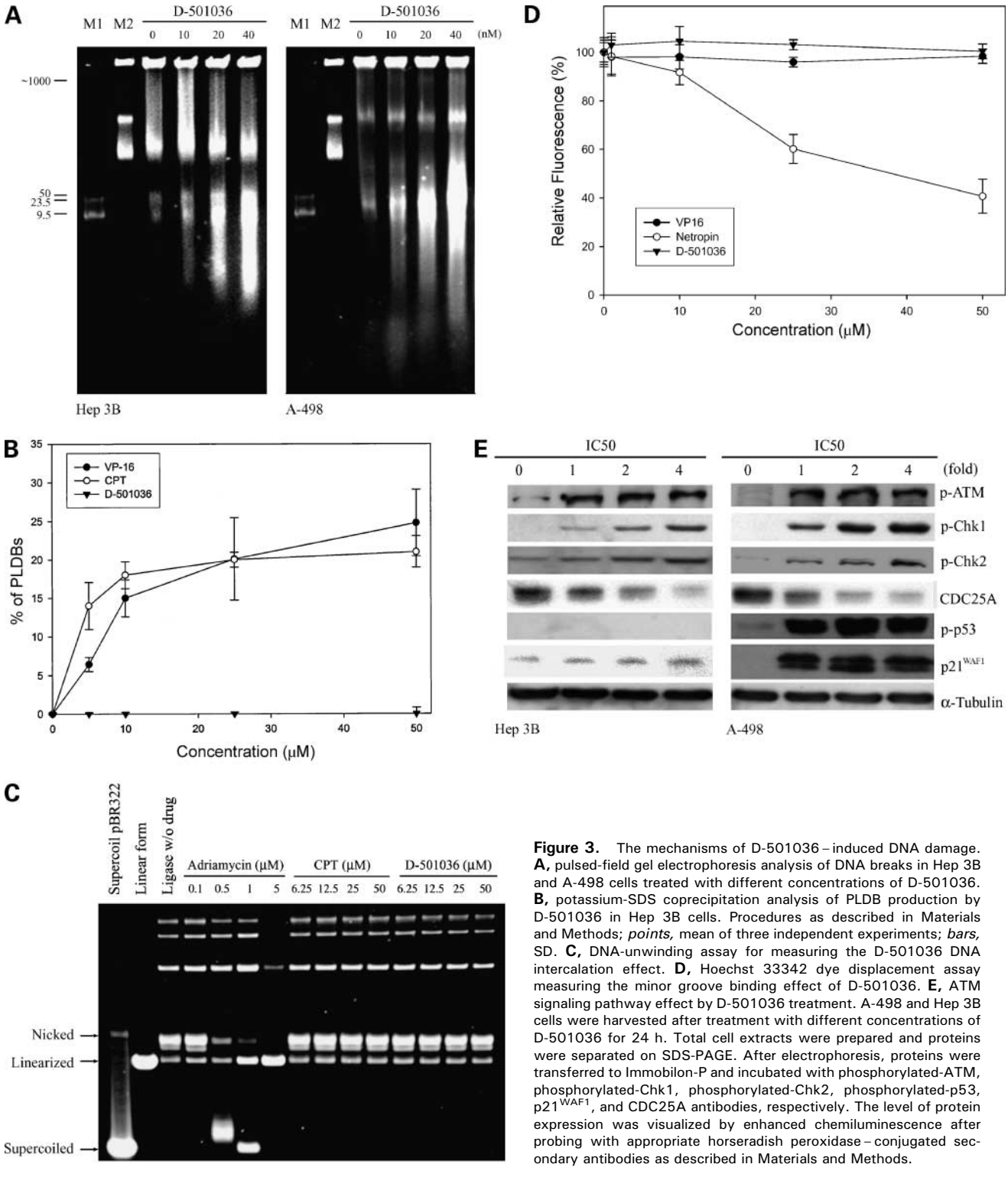

Figure 3. The mechanisms of D-501036 – induced DNA damage. **A,** pulsed-field gel electrophoresis analysis of DNA breaks in Hep 3B and A-498 cells treated with different concentrations of D-501036. **B,** potassium-SDS coprecipitation analysis of PLDB production by D-501036 in Hep 3B cells. Procedures as described in Materials and Methods; *points,* mean of three independent experiments; *bars,* SD. **C,** DNA-unwinding assay for measuring the D-501036 DNA intercalation effect. **D,** Hoechst 33342 dye displacement assay measuring the minor groove binding effect of D-501036. **E,** ATM signaling pathway effect by D-501036 treatment. A-498 and Hep 3B cells were harvested after treatment with different concentrations of D-501036 for 24 h. Total cell extracts were prepared and proteins were separated on SDS-PAGE. After electrophoresis, proteins were transferred to Immobilon-P and incubated with phosphorylated-ATM, phosphorylated-Chk1, phosphorylated-Chk2, phosphorylated-p53, $p21^{WAF1}$, and CDC25A antibodies, respectively. The level of protein expression was visualized by enhanced chemiluminescence after probing with appropriate horseradish peroxidase – conjugated secondary antibodies as described in Materials and Methods.

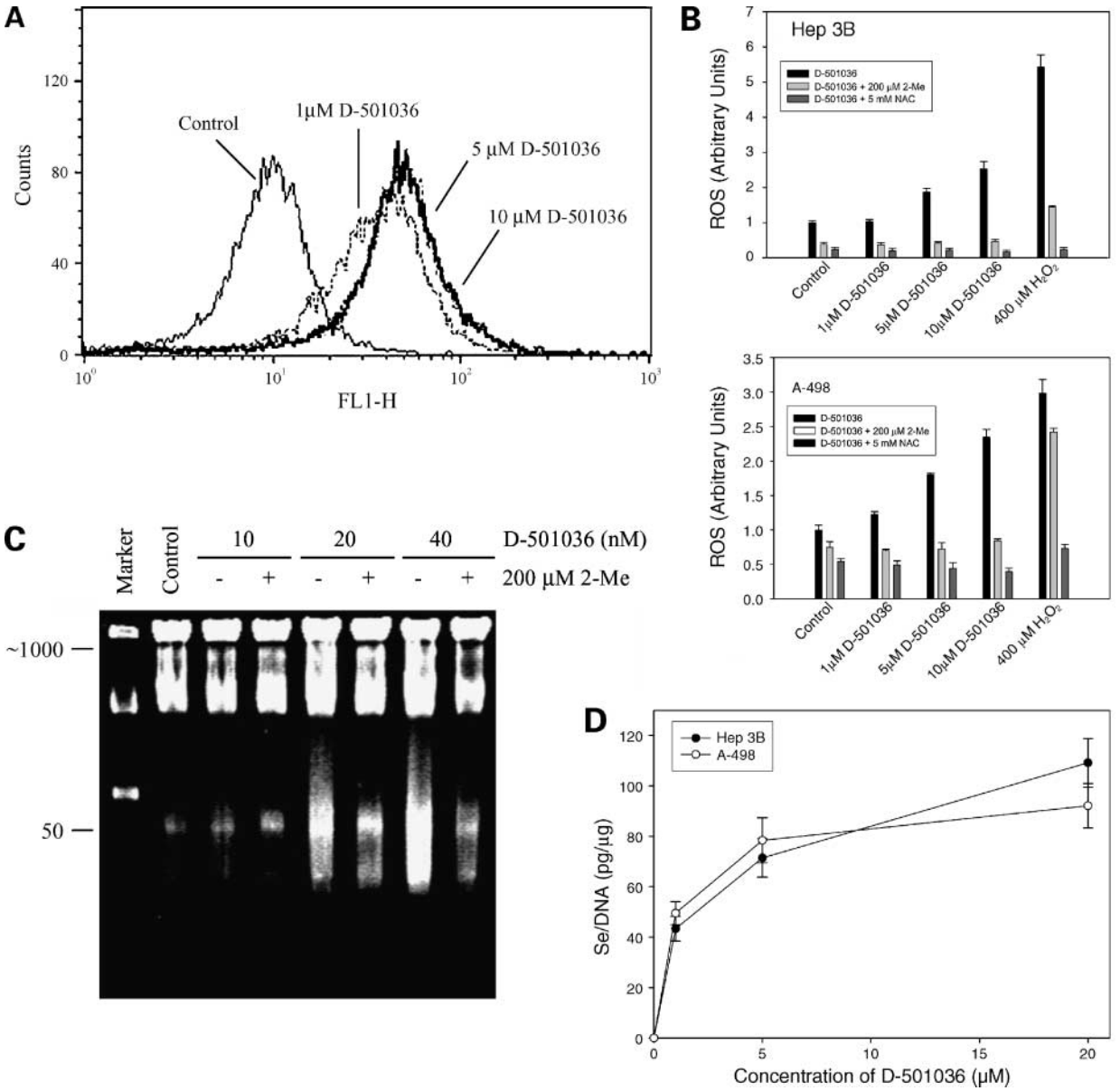

Figure 4. Generation of ROS and DNA adducts by D-501036. **A,** flow cytometry analysis of ROS production of the D-501036–treated A-498. **B,** effect of antioxidant *N*-acetylcystine and β-mercaptoethanol on D-501036–induced ROS production. **C,** effect of β-mercaptoethanol on D-501036–induced DNA break. **D,** dose-response of D-501036–induced Se-DNA adduct formation by inductively coupled plasma–mass spectrometry. *Points,* mean of three independent experiments; *bars,* SD.

Fig. 4B, although D-501036–induced ROS production was completely blocked by the pretreatment of β-mercaptoethanol and *N*-acetylcystine, only a partial reversal of the D-501036–induced DNA breaks was evident (Fig. 4C), suggesting that induction of ROS might not be the sole factor contributing to the D-501036–mediated DNA damage. We therefore investigated whether cocultivation with D-501036 resulted in the formation of DNA adduct in the cells. Our results clearly show that D-501036 induced Se-DNA adduct formation in a concentration-dependent manner in both Hep 3B and A-498 cells (Fig. 4D).

Antitumoral Efficacy of D-501036 in Xenograft Experiments *In vivo*

There was a delay of tumor growth in mice treated with 20 mg/kg of D-501036. Moreover, tumor growth was completely abrogated when the mice were treated with 50 mg/kg of D-501036 for the entire period of observation (Fig. 5A). The tumor-free condition of these mice persisted for >12 weeks after discontinuance of the treatment (data not shown). There was <10% of body weight loss observed in all mice treated with D-501036 and body weight regained after the treatment was terminated (Fig. 5B).

Discussion

In previous studies, we focused on the design and synthesis of a series of selenium-containing polythiophene analogues. Several selenophene compounds synthesized in our laboratory have been shown to possess potent inhibitory ability against tumor growth. Nevertheless, the properties of poor solubility and stability, similar to the terthiophene, impede their further development. To improve solubility and stability, *N*-methylpyrrole with one or more hydroxymethyl groups were systematically introduced to the original selenophene compounds. One of these novel compounds, D-501036, showed potent antitumor activity with better solubility and stability, and was thus chosen for further development.

In this study, we show that D-501036 is a potent antiproliferative agent against various models of human solid tumor derived from different organs. The IC_{50} values for D-501036 for the cell lines Hep 3B (hepatocellular carcinoma), A-498 (renal carcinoma), MCF-7 (breast carcinoma), NPC-TW01 (nasopharyngeal carcinoma), LNCaP (prostate carcinoma), and NCI-H460 (non–small cell lung cancer) were ~3 to 50 nmol/L (Table 1). Despite its highly antiproliferative activity against human cancer cells, D-501036 displays almost nontoxic activity toward three normal human cells, including renal proximal tubular (RPTEC), bronchial epithelial (NHBE), and skin fibroblast (Detroit 551) cell lines, suggesting that D-501036 possesses great selectivity between normal and cancer cells. Moreover, D-501036 was also shown to be equally effective against two KB-derived MDR-positive cell lines despite their P-gp170/MDR status (Table 2), suggesting D-500136 is a poor substrate of P-gp170/MDR.

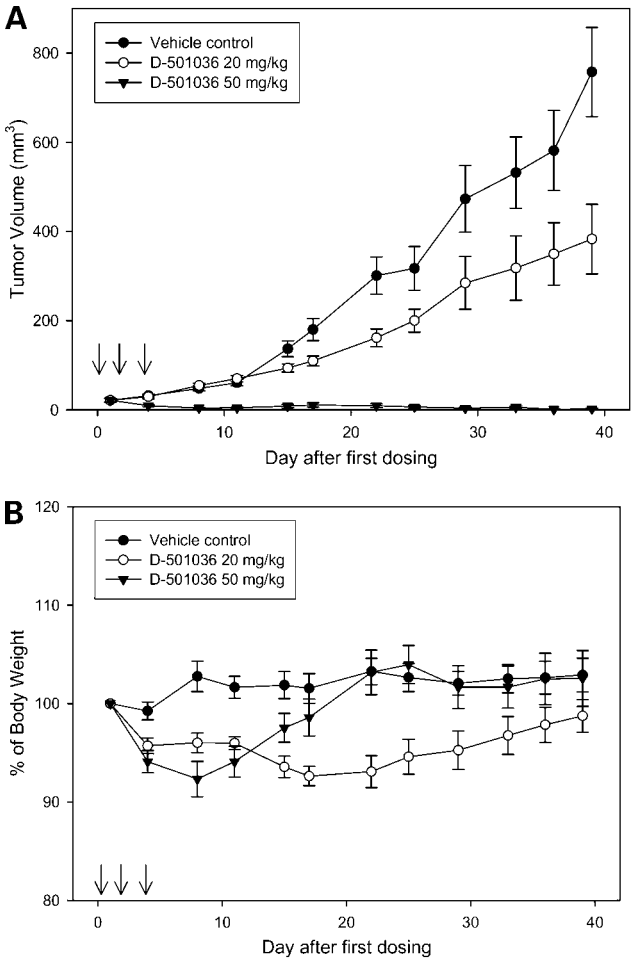

Figure 5. Inhibition of A-498 tumor growth in the mouse xenograft model by D-501036. Nude mice bearing human renal carcinoma A-498 xenografts were treated with vehicle control, 20 mg/kg, and 50 mg/kg of D-501036 i.p. thrice every other day. Tumor size and body weight of mice were measured twice a week. **A,** *points,* mean tumor volume (mm^3) at each time point; *bars,* SD. **B,** *points,* mean relative body weight (%) at each time point; *bars,* SD. *Arrows,* day of i.p. injections.

To identify the molecular targets which are critical to D-501036 antiproliferative activity, several pathways have been investigated. In contrast to previous findings that the growth inhibitory activity of α-terthiophene derivatives might be partially through the inhibition of PKC-α and PKC-β2 enzymatic activity (2), our data clearly shows that D-501036 has no inhibitory activity against PKC-α and PKC-β2 (Fig. 1), suggesting that the antiproliferative activity of D-501036 was not attributable to the inhibition of PKC-α and PKC-β2 function.

Of note, D-501036 exhibits a low level of resistance toward the VP16-resistant KB variant, KB-7D, in a growth inhibition assay (Table 2), which shows a down-regulation of topoisomerase II and overexpression of multidrug-resistant protein (5). In addition, cell cycle analyses shows that D-501036 treatment results in a concentration-dependent accumulation in the S phase with concomitant losses of G_0-G_1 and G_2-M phases in both Hep 3B and A-498 cells (Fig. 2A). Moreover, several lines of evidence have shown that selenium could induce cellular apoptosis via the induction of topoisomerase II cleavage product (13), and activation of p53 (14). Therefore, we hypothesized that D-501036 might cause DNA damage and lead to cell death. The results of pulsed-field gel electrophoresis analyses show that D-501036 could indeed cause DNA breaks with the induction of 50 to 300 kb fragmentation in a concentration-dependent manner in both Hep 3B and A-498 cells (Fig. 3A). However, in contrast to the induction of PLDBs by camptothecin (Topo-I poison) and VP16 (Topo-II poison), no PLDBs generated by D-501036 were found (Fig. 3B). We also showed that D-501036 could not generate Topo-I or Topo-II–mediated DNA breaks (data not shown). Furthermore, our unwinding and minor groove binding assays show that D-501036 is neither intercalating nor binding to the minor groove of DNA (Fig. 3C and D). Taken together, our results suggest that D-501036–induced DNA breakage is not mediated via either Topo-I or Topo-II or DNA binding.

Apoptosis induced by DNA-damaging agents has been associated with the activation of either the ATM or Rad-3–related protein kinase gene (15–17). Our data is consistent with the scenario that D-501036–induced DNA damage can activate ATM, subsequently leading to hyperphosphorylation of Chk1, Chk2, and p53, decreased expression levels

of CDC25A, and up-regulation of $p21^{WAF1}$ in both p53-deficient (Hep 3B) and p53-proficient (A-498) cells (Fig. 3E). These results show that D-501036–induced cell death is associated with, at least, ATM activation and p53-dependent and p53-independent apoptosis pathways.

Previous reports have shown that sodium selenite as well as methylated forms of selenium could induce apoptosis through the induction of oxidative stress (18) and generation of the DNA adduct (19). We first determined whether D-501036 could induce ROS and cause DNA damage subsequently. Our data show that the levels of ROS in D-501036–treated Hep 3B and A-498 cells increase rapidly in a concentration-dependent manner (Fig. 4A). Nevertheless, pretreatment of cells with antioxidants could completely block D-501036–mediated ROS production, but only partially reverse the D-501036–induced DNA breaks (Fig. 4C), suggesting that ROS production is not the only factor contributing to D-501036–mediated DNA damage. We further found Se-DNA adduct formation in both Hep 3B and A-498 cells treated with D-501036 in a concentration-dependent manner (Fig. 4D). Although the nature of D-501036–induced DNA adducts is under investigation, our data indicates that both ROS production and DNA adduct formation contribute to D-501036–induced DNA damage. Whether D-501036 directly induces a rapid DNA double-strand break or creates a lesion that arrests DNA replication, triggers the apoptosis signaling pathway, and in turn, is converted into a DNA double-stand break has not been clarified here, however, these issues are being investigated.

In conclusion, our data shows for the first time that D-501036, a novel selenophene-based triheterocyclic derivative, possesses potent activity against various human solid tumor cells. Both induction of ROS and formation of Se-DNA adducts contribute to D-501036–induced DNA damage, which leads to the activation of the ATM signaling pathway. The activation arrests cells in S phase and subsequently triggers tumor cell apoptosis through p53-dependent and p53-independent pathways. Furthermore, D-501036 exhibits strong antitumor activity *in vivo*. These findings indicate that D-501036 is a promising novel polyselenophene compound with potential for the treatment of human cancers.

References

1. Cragg GM, Newman DJ, Weiss RB. Coral reefs, forests, and thermal vents: the worldwide exploration of nature for novel antitumor agents. Semin Oncol 1997;24:156 – 63.

2. Kim DS, Ashendel CL, Zhou Q, Chang CT, Lee ES, Chang CJ. Novel protein kinase C inhibitors: α-terthiophene derivatives. Bioorg Med Chem Lett 1998;8:2695 – 8.

3. Chang Cj, Ashendel CL, Chan TCK, Geahlen RL, McLaughlin JL, Waters DJ. Oncogene signal transduction inhibitors form Chinese medicinal plants. Pure Appl Chem 1999;71:1101 – 4.

4. Combs GF, Jr., Gray WP. Chemopreventive agents: selenium. Pharmacol Ther 1998;79:179 – 92.

5. Kuo CC, Hsieh HP, Pan WY, et al. BPR0L075, a novel synthetic indole compound with antimitotic activity in human cancer cells, exerts effective antitumoral activity *in vivo*. Cancer Res 2004;64:4621 – 8.

6. Goueli BS, Hsiao K, Tereba A, Goueli SA. A novel and simple method to assay the activity of individual protein kinases in a crude tissue extract. Anal Biochem 1995;225:10 – 7.

7. Rowe TC, Chen GL, Hsiang YH, Liu LF. DNA damage by antitumor acridines mediated by mammalian DNA topoisomerase II. Cancer Res 1986;46:2021 – 6.

8. Camilloni G, Della SF, Negri R, Grazia FA, Di ME. Structure of RNA polymerase II promoters. Conformational alterations and template properties of circularized *Saccharomyces cerevisiae* GAL1-10 divergent promoters. EMBO J 1986;5:763 – 71.

9. Montecucco A, Pedrali-Noy G, Spadari S, Zanolin E, Ciarrocchi G. DNA unwinding and inhibition of T4 DNA ligase by anthracyclines. Nucleic Acids Res 1988;16:3907 – 18.

10. Yamori T, Matsunaga A, Sato S, et al. Potent antitumor activity of MS-247, a novel DNA minor groove binder, evaluated by an *in vitro* and *in vivo* human cancer cell line panel. Cancer Res 1999;59:4042 – 9.

11. Shen HM, Shi CY, Shen Y, Ong CN. Detection of elevated reactive oxygen species level in cultured rat hepatocytes treated with aflatoxin B1. Free Radic Biol Med 1996;21:139 – 46.

12. Juang SH, Pan WY, Kuo CC, et al. A novel bis-benzylidenecyclopentanone derivative, BPR0Y007, inducing a rapid caspase activation involving upregulation of Fas (CD95/APO-1) and wild-type p53 in human oral epidermoid carcinoma cells. Biochem Pharmacol 2004;68:293 – 303.

13. Zhou N, Xiao H, Li TK, Nur-E-Kamal A, Liu LF. DNA damage-mediated apoptosis induced by selenium compounds. J Biol Chem 2003;278:29532 – 7.

14. Jiang C, Hu H, Malewicz B, Wang Z, Lu J. Selenite-induced p53 Ser-15 phosphorylation and caspase-mediated apoptosis in LNCaP human prostate cancer cells. Mol Cancer Ther 2004;3:877 – 84.

15. el-Deiry WS, Tokino T, Velculescu VE, et al. WAF1, a potential mediator of p53 tumor suppression. Cell 1993;75:817 – 25.

16. Zhu H, Zhang L, Wu S, et al. Induction of S-phase arrest and p21 overexpression by a small molecule 2[[3-(2,3-dichlorophenoxy)propyl] amino]ethanol in correlation with activation of ERK. Oncogene 2004;23:4984 – 92.

17. Gartel AL, Tyner AL. The role of the cyclin-dependent kinase inhibitor p21 in apoptosis. Mol Cancer Ther 2002;1:639 – 49.

18. Shen HM, Yang CF, Ong CN. Sodium selenite-induced oxidative stress and apoptosis in human hepatoma HepG2 cells. Int J Cancer 1999;81:820 – 8.

19. Stewart MS, Spallholz JE, Neldner KH, Pence BC. Selenium compounds have disparate abilities to impose oxidative stress and induce apoptosis. Free Radic Biol Med 1999;26:42 – 8.

Molecular Cancer Therapeutics

D-501036, a novel selenophene-based triheterocycle derivative, exhibits potent *in vitro* and *in vivo* antitumoral activity which involves DNA damage and ataxia telangiectasia–mutated nuclear protein kinase activation

Shin-Hun Juang, Chia-Chi Lung, Pi-Chen Hsu, et al.

Mol Cancer Ther 2007;6:193-202.